The Lipid-related Effects of Resveratrol on Human Ectopic Endometrial Stromal Cells and a Rat Model of Endometriosis

Zhengyun Chen
Zhejiang University School of Medicine Women's Hospital
Chunyan Wang
Zhejiang University School of Medicine Women's Hospital
Cuicui Lin
Zhejiang University School of Medicine Women's Hospital
Lifeng Zhang
Zhejiang University School of Medicine Women's Hospital
Huimei Zheng
Zhejiang University School of Medicine Women's Hospital
Yong Zhou
Zhejiang University School of Medicine Women's Hospital
Xiaoyong Li
Zhejiang University School of Medicine Women's Hospital
Chen Li
Zhejiang University School of Medicine Women's Hospital
Xinmei Zhang
Zhejiang University School of Medicine Women's Hospital
Xiaohang Yang
Zhejiang University School of Medicine Women's Hospital
Minxin Guan
Zhejiang University School of Medicine Women's Hospital
Yongmei Xi (xyyongm@zju.edu.cn)
Zhejiang University School of Medicine https://orcid.org/0000-0001-7374-2564

Research

Keywords: Endometriosis, Ectopic endometrial stromal cells, Resveratrol, Lipid metabolism, PPARα, Rat model

Posted Date: November 19th, 2020

DOI: https://doi.org/10.21203/rs.3.rs-110546/v1

Abstract

Background: Endometriosis is a complex disease in the field of gynecology that has certain limitations for its interim treatment. Resveratrol has been recently used for the treatment of endometriosis in experimental and clinical studies, but its molecular mechanism remaines elusive.

Results: In this study, based on a case-control study, we identified that a decreased BMI and altered lipid profiles were associated with endometriosis patients. We applied resveratrol treatment on human ectopic endometrial stromal cells (HEcESCs) and a rat model of endometriosis. Lipidomics analysis showed that resveratrol altered lipid profiles in HEcESCs, with the sphingolipids Cer and SM increased significantly, while FA and most phospholipids were significantly reduced. Pathway enrichment analysis showed that several lipid-associated signaling pathways could be targeted by resveratrol. Our experiments in a rat model showed that resveratrol reduced the lesion and rectified lipid profiles in rats with endometriosis. In addition, resveratrol treatment significantly increased the expression of PPARα in lesion tissues of model rats and HEcESCs of EMs patients.

Conclusion: Our data reveal that the development of EMs is closely related to lipid metabolism, and resveratrol may play a therapeutic role by targeting the lipid metabolism of ectopic endometrial stromal cells in endometrosis. Our study provides valuable insights for understanding the pathogenesis and clinical treatment of endometriosis.

Background

Endometriosis (EMs) is an estrogen-dependent chronic inflammatory disease. It is associated with functional endometrial glands and stroma implantation outside the uterus. Women with EMs often suffer from severe pelvic pain, resulting in significantly decreased quality of life and high costs for the health-care system (1). The diagnosis of EMs relies solely on laparoscopy, from which three phenotypes can be identified; superficial peritoneal endometriosis (SUP), ovarian endometriosis (OMA), and deep infiltrating endometriosis (DIE), according to location and lesion size (2, 3). With no useful biomarkers yet established, such laparoscopic discoveries may take place 8–11 years after the actual onset of the disease. Currently available treatments include surgery and hormone medication which have many unpleasant side effects and a high rate of relapse beyond their completion (4). Limitations and complications relating to interim treatment are largely due to incomplete understanding of the underlying mechanism.

Patients with EMs often show low body mass index (BMI) and unfavorable serum lipid profiles (5), while patients with BMI < 18.5 kg/m2 are more likely to be associated with severe disease phenotypes (6). Correspondingly, high levels of serum Lp(α), TG, and ApoA1, but not LDL-C or HDL-C, have been identified in EMs patients (7). Another cross-sectional study (N = 120) demonstrated that an elevation of serum LDL, but non-HDL and TC, was identified in patients with EMs, as compared with control women (8). The key components of plasma lipids play central roles in varied metabolic diseases. LDL-C delivers fat

molecules to cells and HDL-C promotes cholesterol efflux from cells (9). Gene expression analysis revealed that LDL receptors were highly expressed in endometrial tissues of patients with DIE (10). ApoA1 mediates the exchange between HDL and chylomicron and functions as a regulator of inflammatory responses (11). These studies indicated that there may be some strong links between the disorders of fat digestion and absorption, and the inflammation in the patients with EMs. We have previously investigated rutine metabolite parameters of EMs patients using enzymatic colorimetric assays or the immune turbidimetric methods, attempting to find potential indicators that can be used to detect the EM phenotype (12). However, such serum metabolites index seemed to be lack of specificity and sensitivity for the diagnosis of EMs.

Recently, lipidomics analysis has been widely used to assess lipid homeostasis in various tissue samples (13, 14). In such studies, elevated levels of SM, PC and TG were identified in serum samples of OMA patients (15). Significant alterations in SM, PC, TG and PE between the eutopic and ectopic endometrium were also noted in patients with EMs (16, 17). As a direct infiltration environment for ectopic endometrium, peritoneal fluid in patients with EMs was found to have a decreased PC level (18, 19). Such lipidomics analysis data has been mostly targeted to find biomarkers for the clinical detection of this disease. Although these observations indicate that abnormal lipid distribution may play a major role in pathology related to EM, little attention has been given towards the potential application of lipidomics analysis in evaluating drug efficacy or further elucidating disease mechanisms. Rresveratrol (trans-3,5,4’-trihydroxystilbene), a phytoalexin polyphenol found in natural plants or fruits, has previously been highlighted as a potential supplement for the treatment of cancers, cardiovascular disease and EMs (20, 21). The pharmacological effects of resveratrol on energy and lipid metabolism have been revealed in animal models or in human eutopic endometrial stromal cells (HESCs) of EMs (22). Resveratrol intervention also led to a decrease in total cholesterol and triacylglycerol concentrations in individuals with dyslipidemia (23, 24). The lipid-related effects of resveratrol on HEcESCs and animal model of EMs is no known.

In the present study, based on analysis of metabolic indicators in clinical cases, we identified that a decreased BMI and abnormal lipid metabolism is strongly associated with the development of endometriosis. Using lipidomics analysis, we evaluated the effect of resveratrol on HEcESCs. Therapeutic effect of resveratrol on EMs model rats were also observed, showing with atennuated lesion size and rectified lipid profiles. Our study provides valuable insights towards the understanding of pathologenesis of EMs and reveals the potential of resveratrol for the treatment of patients with endometriosis.

Results

Decreased BMI and altered serum lipid profiles in EMs patients

In a case-control study (n = 205), we assessed the clinical characteristics and serum metabolic profiles in women with or without EMs. 110 patients were histologically confirmed with EMs and 95 EMs-free

women served as the control group. According to the phenotypes, the EMs patients were sub-grouped as 79 OMA and 31 DIE. The patient's distribution according to the r-ASRM stage was 46 moderate and 64 severe. Among controls, the indications for surgery were summarized as benign ovarian tumors (41 cases), tubal infertility (13 cases), cervical intraepithelial neoplasia (28 cases), and intrauterine adhesion (13 cases). There were no significant differences in age, parity, and gravidity across the different groups. However, univariate analyses revealed that the BMI in all patients with Ems and in patients with OMA were significantly lower than those of control. However, there were no significant differences with respect to serum TC, TG, LDL, HDL, Lp(α) and UA levels between EMs and control patients. Strikingly, elevated levels of R-ApoA1/ApoB and decreased levels of R-ApoB/ApoA1 and serum FBG were displayed in all EMs patients as compared with controls (Table. 1). With respect to the EMs phenotypes, serum R-ApoA1/ApoB levels were both significantly higher in OMA and DIE patients, as compared to controls. Elevated serum Lp(α) and a decreased FBG levels were observed in OMA patients but not in DIE patients, when compared to controls. There was also significant differences in Lp(α) levels between OMA patients and DIE patients (Table. 1).

A stepwise logistic regression analysis showed that BMI was associated with a decreased chance, whereas Lp(α) and R-ApoA1/ApoB was associated with an increased risk of OMA. As for DIE, only R-ApoA1/ApoB showed a strong association with the phenotype (Table 2). Diagnostic performances of BMI and serum lipid profiles for EMs were also predicted using ROC analysis. The area under the curve (AUC) for R-ApoA1/ApoB could as a single biomarker of EMs with good specificity and relative low sensitivity (Fig. S1). These data indicated that an abnormal lipid metabolism was strongly associated with the development of EMs.

Lipidomics analysis on the HEcESCs upon resveratrol treatment

With permission, we isolated HEcESCs of lesion samples obtained from 8 EMs patients. The cultured primary HEcESCs treated with resveratrol for 48 hours (Res groups), together with those treated with DMSO as controls (Con groups), were subjected to lipid extraction and non-target lipidomics analysis by UPLC-MS. Based on the OSI/SMMS lipid library, 809 qualitative lipid structures were differentially classified, mainly including 5 types of glycerophospholipids (PC, PE, PG, PS, PI), 4 types of sphingolipids (SM, Cer, HexCer, Hex2Cer), 3 types of glycerolipids (MG, DG, TG) and FA. 638 lipids under the positive ions model and 313 lipids under the negative ions model were recognized. Among these, 132 lipids were identified in both ion models. Comparing the peak value of differential lipids between the Res groups and Con groups, 63 lipids were quantified as significantly altered candidates upon resveratrol treatment ($P < 0.05$, $FC > 1.5$, $VIP > 1$). Using One-MAP (www.5omics.com), univariate data analysis showed the overall metabolite features with differential variations among samples of the paired groups (Res vs Con). PE (16:0p-18:2), SM (18:0/18:0), PC (18:0–18:1), FA (13:0/14:1/15:0/15:1), PI (17:2/18:1) and Cer (d18:1/14:0), were significantly altered in the Res group (Fig. 1A). The lipid changes between the paired groups were also showed with a Z-scores plot (Fig. 1B). In particular, the sphingolipids (such as Cer, SM)

showed obvious upregulation, and glycerolipids (such as DG, TG), FA, and most of the phospholipids including PC, LPC, PE, LPE, PG, PI, PS, showed significant down regulation (Fig. 1C and Table. S1).

Multivariate statistical analysis showed that there was an obvious separation trend between the Res group and Con group, firstly revealed in the PCA model (Fig. 2A). The two groups were then significantly distinguished in the supervised models PLS-DA and O-PLS-DA (Fig. 2B and 2C). ROC analysis showed a high quality of the predictive value (AUC = 1) (Fig. 2D). The perturbative index (R2 × 0 = 0.29, Q2 × 0=-0.26) indicated that the model had good predictability and reliability (Fig. 2E). Among all the lipids altered after resveratrol treatment, PI (15:1–16:2) showed the most variation contributing to the separation between the two groups, with a highest VIP (VIP = 2.88) (Fig. 2F).

Resveratrol-mediated changes in lipid-associated signaling pathways

The above altered lipid metabolites (under criteria either VIP > 1, P < 0.05 or FC > 1.5) were subjected to the KEGG database for pathway enrichment analysis. As shown in Fig. 3A, the lipidomic alterations upon resveratrol treatment were mostly assigned to the glycerophospholipid metabolism, insulin resistance (IRS) and sphingolipid signaling pathways, among all related pathways (Table. S2). Resveratrol could inhibit the synthesis of cholesterol and the downregulation of apolipoproteins (24). The phospholipids PE, PC and PI were significantly reduced upon resveratrol treatment (Fig. 3B), which might result in a decreased synthesis of PI and PG in glycerophospholipid metabolism pathways and an activation of IRS pathways. Significantly, downregulation of FA (Fig. 3C) had affects upon the cholesterol metabolism and IRS pathways. Significant upregulation of Cer and SM (Fig. 3D) might be involved in the sphingolipid metabolism pathway.

We next examined the effects of resveratrol on the lesion cells obtained from patients. Three groups of HEcESCs treated with or without resveratrol were subjected to the assays for evaluation of cell proliferation, invasiveness and apoptosis. After 48 hours treatment with resveratrol at different concentrations (40 μM and 100 μM), the proliferation capacity of the HEcESCs had decreased in the Res-40 μM group and Res-100 μM group compared with the control groups (Fig. 4A). In the invasiveness assay, the number of cells crossing the matrigel differed significantly with resveratrol treatment at a concentration of 40 μM or 100 μM, which were decreased respectively, compared with the control group (Fig. 4B and 4C). The effects of resveratrol on the apoptosis of HEcESCs were shown in Fig. 4D, both Res-40 μM and Res-100 μM showed significant differences (Fig. 4E).

Lipid profil varys with the severity of endometriosis in a rat model.

We firstly generated a rat model of EMs by autologous transplantation of rat estrus epithelial tissue into the endometrial abdominal wall (Fig. 5A and 5A') to test the therapeutic effects of resveratrol. Examined after 4 weeks of modelling, successful implants showed EMs-like lesions appearing as vesicular cysts

(Fig. 5A and 5A”), filled with clear or turbid yellow-brown liquid and surrounded by connective tissue and angiogenesis (Fig. 5A and 5A‴). HE staining showed that the pathological features of implant-derived ectopic endometrium shared similarities to the eutopic endometrium (Fig. 5B and 5C).

To further evaluate the pathological characteristics of the model rats, we examined the serum metabolites including cholesterol, HDL, LDL and TG of the model rats and the sham group of animals. We evaluated the relationship between lesion size and the lipid levels in the serum. The EMs model animals were classified into three levels according to severity (n = 10 in each group): EMs 1: 2 $mm^3 \leq$ lesion volume < 20 mm^3, EMs 2: 20 $mm^3 \leq$ lesion volume < 100 mm^3, EMs 3: lesion volume $\geq$ 100 mm^3. Compared to the sham group, in EMs 1 group, there were no significant differences in serum cholesterol (Fig. 5D), HDL (Fig. 5E), LDL (Fig. 5F) and TG (Fig. 5G). In both EMs 2 and EMs 3 groups ($\geq$ 20 mm^3), the levels of serum cholesterol, HDL, LDL but not TG were significantly increased (Fig. 5D-5G). These data indicated a positive correlation between the serum levels of cholesterol, HDL and LDL and lesion severity in the model rats.

We applied animal open field assay to evaluate the anxiety of rats with EMs that were likely associated with increased stress or pain. This experiment was often used as test for anxiety, exploration, and locomotion and the behavioral responses could be scored by measuring the time spent in the center zone and numbers of center crossing (25). The results indicated that the EMs group showed more anxiety than the control group (Fig. S2A and S2B), with significant decreases in the time spent in the center area (Fig. S2C) and frequency of entering the central area (Fig. S2D) .

Resveratrol attenuated the lesion size and aberrant lipid profiles of the EMs model rats

Resveratrol were applied for intraperitoneal injection in the experimental rats, after 4 weeks, the ectopic endometrial lesions of the animal models treated with or without resveratrol were examined. Compared to the EMs group without resveratrol treatment (Fig. 5H and 5I), significant reduction of lesion sizes were shown in both Res-med groups and Res-high groups (Fig. 5J). The pathological lesions of EMs are typically characterized by the histological accumulation of endometrial epithelial, glandular tubes, and significant invasive growth (26). Histochemical staining showed that resveratrol treatment led to both significant decreases in glandular tubes and endometrial epithelial thickness in both Res-med groups and Res-high groups (Fig. 5K), compared to the EMs group without resveratrol treatment (Fig. 5K’ and 5K”).

After resveratrol treatment for 4 weeks, we measured the serum cholesterol (Fig. 6A), HDL (Fig. 6B), LDL (Fig. 6C), and TG (Fig. 6D) of model rats. Results showed that the levels of cholesterol, HDL, LDL in the Res-med group, and the levels of cholesterol, HDL but not LDL in the Res-high group were significantly decreased, compared to the EMs group without such treatment (Fig. 6A-6C). No significant changes in TG levels occurred among these groups (Fig. 6D). These data suggested that resveratrol treatment has efficacy to rectify the aberrant lipid profiles in EMs model rats. As the occurrence of EMs had been previously shown to be related to cell adhesion, angiogenesis and apoptosis in a mouse model, we

extracted mRNA from lesion tissues to analyze the corresponding molecules such as MMP-2, ICAM-1, VEGF and BCL-2 (27), and evaluated any expression alterations associated with resveratrol. Results showed that the mRNA expression of MMP-2 (Fig. 6E), VEGF (Fig. 6F) and BCL-2 (Fig. 6G), but not ICAM-1 (Fig. 6H) were significantly increased in lesion tissues of the EMs group as compared to the Sham group (Fig. 6E-6H). After resveratrol treatment, the mRNA expressions of MMP-2, VEGF and BCL-2 (Fig. 6G), but not ICAM-1 (Fig. 6H) were significantly decreased, compared to the EMs group (Fig. 6E-6H). These observations indicated that, in addition to the reduction of lesion size upon resveratrol treatment in the model rats, there were also associated decreases in cell invasion and angiogenesis and increased apoptosis.

Resveratrol induces PPARα expression in both HEcESCs and EMs model rats

Resveratrol has been previously shown to stimulate PPARα activation that suppresses the transcriptional activity of metabolic genes involved in energy and lipid metabolism homeostasis in endothelial cells (28, 29). We analyzed the mRNA levels of PPARα in HEcESCs and in ectopic endometrial tissues of the model rats upon resveratrol treatment. Results showed that mRNA expression of PPARα was significantly increased in either HEcESCs (Fig. 6I) or model rats (Fig. 6J). The protein levels of PPARα were analyzed using the ectopic endometrial tissues of model rats (EMs) and the lesion samples obtained from the model rats were treated with either medium or high dosage of resveratrol. An increased PPARα expression was detected in the lesion tissues of model rats treated with resveratrol, compared to the untreated EMs groups (Fig. 6K and 6L). These observations suggested that resveratrol treatment had resulted in lesion attenuation in model rats and that apoptosis in HEcESCs might occur via PPARα activation.

Discussion

EMs is a refractory disease that affects approximately 10% of women of reproductive age and up to 50% of women with infertility. Immune deficiency, heightened oxidative stress, and systemic chronic inflammation have been considered as critical facilitators in disease progression (30). The heterogeneity of the disease, having different stages and phenotypes, makes timely and accurate diagnosis of EMs a considerable clinical challenge. In the present study, we evaluated metabolite profiles as risk factors and potential biomarkers for EMs phenotypes. In doing so, we highlight the critical involvement of the lipid metabolism in the progression of EMs. This may help identify patients at risk of developing this disease and aid in treatment decisions based on lipid profiles.

Resveratrol has been shown to inhibit the development of EMs using a nude mouse model where it reduced the invasiveness of eutopic endometrial stromal cells (31). Our study showed that the treatment of resveratrol led to the inhibition of cell proliferation and invasiveness and the promotion of apoptosis in HEcESCs. We further demonstrated that upon resveratrol treatment, glycerolipids such as FA, DG and TG and most phospholipids showed significant downregulation, particularly those involved in the cholesterol metabolism and insulin resistance pathways (Fig. 7). Sphingolipids such as SM and Cer have been

demonstrated to have inhibitory effects on colon cancer, suppressing cell proliferation (32, 33). In our experiments of resveratrol treatment in HEcESCs, increased SM and Cer were also observed along with the inhibition of cell proliferation (Fig. 4A and Fig. 7). These lipids are key components of the plasma membrane and other cellular compartments that integrate into many biological processes such as those of signaling pathways, wound healing and anti-inflammation. Such lipidomic alterations may form a dynamic network contributing to pathologies associated with EMs.

PPARα responds to fatty acid signals derived from dietary lipids, pathogenic lipoproteins or essential fatty acid metabolites and thereby controls both the lipid metabolism and inflammation (34). Resveratrol stimulated PPARα activation has been reported to be associated with an increased phosphorylation of AMPK in human glomerular endothelial cells (35). In our study, lipidomics analysis of HEcESCs treated with resveratrol also showed a significant activation of PPARα, probably through an up-regulated AMPK signaling and PGC1 pathway. Resveratrol mediated down-regulation of DAG might directly activate IRS/PI3K-AKT pathways (Fig. 7). PPARα-mediated changes in the FA and AMPK pathways eventually resulted in regulating lipid transport genes, such as ApoA1 and ApoA2 (Fig. 7). Therefore, resveratrol might act as an agonist for PPARα and interplay with lipid-associated pathways, together contributing to recovery from EMs. Further investigation is required to confirm the possible role of PPARα as a molecular target for the treatment of EMs.

As a chronic inflammatory disease, both the onset and recovery phases of EMs may be closely related to the status of lipid metabolites. Lipids can function in tissue remodelling and act to maintain homeostasis during inflammatory processes (36). Lp(α) acts as an acute phase protein with a pro-inflammation role and is active in the modulation of tissue repair in cases of injury (9). ApoA1 has anti-inflammatory properties and also can act as a phase protein involved in wound healing (37, 38). Both ApoA1 and ApoB are involved in cholesterol traffic (39). Our study revealed that imbalanced R-ApoA1/ApoB may function as a specific suppressor of inflammatory responses in EMs cases which is also present as a risk factor to facilitate the abnormal survival of endometrial tissue. In addition, an increased serum Lp(α) level as an independent risk factor for the OMA phenotype may indicate the critical effect of inflammation and pro-atherosclerosis towards the development of EMs. In the model rats, serum levels of cholesterol, HDL and LDL showed significant increases in a lesion size-dependent manner, and subsequent significant decreases upon resveratrol treatment. These data manifested a critical involvement of lipid metabolites in EMs and the therapeutic efficacy of resveratrol targeting of the lipid metabolism.

Conclusion

This comprehensive study shows that the development of EMs is strongly correlated to lipid metabolism, and resveratrol may play a therapeutic role by targeting the lipid metabolism of ectopic endometriotic endometrial stromal cells. Our study provides valuable insights for understanding the pathogenesis and clinical treatment of endometriosis.

Methods

Participants

Patients who were diagnosed having EMs, requiring surgical treatment and referred to the general gynecology department of the Women's Hospital, Zhejiang University School of Medicine, were included in the study. Written informed consent was obtained from each patient before study inclusion. A total of 205 women with EMs (110 cases) and without EMs (95 cases) were enrolled. Indications for surgery in the EMs group were as follows: pelvic mass, history of infertility, pelvic pain, and failed analgesics. Study inclusion criteria of the EMs group included: (1) Age ≤ 40 years; (2) histologically proven EMs; (3) restriction of samples to those of moderate or severe disease (stages 3 and 4) according to the r-ASRM Classification; (4) restriction to OMA or DIE phenotypes (SUP, OMA and DIE phenotypes are frequently associated with each other), with the final phenotypic diagnosis of EMs designated according to the worst lesion, as per a previous study (6). Exclusion criteria were: (1) women with only a SUP phenotype; (2) irregular menstrual cycles; (3) those with history of metabolite diseases such as diabetes, obesity, cardiovascular disease or thyroid disease etc; (4) those with a history of autoimmune or inflammatory diseases; (5) pregnancy; (6) those having had hormone treatment such as oral contraceptives, GnRH analogues or any other hormone treatment during the previous 3 months before the study.

Women ≤ 40 years old requiring surgical treatment, but without any evidence of EMs, were recruited as controls during the same period. Detailed history, a thorough physical examination of the abdominopelvic cavity and sonography screenings were performed by the designated experts for every patient. Control patients presenting with dysmenorrhea or tenderness in the pelvic area or a mass in ovary or those with history of metabolite diseases such as diabetes, obesity, cardiovascular disease or thyroid disease were excluded.

Measurement of serum metabolites

Weight and height was determined for all patients. The BMI was calculated as weight (kg) divided by the square of height (m^2). Venous blood samples were obtained from each patient at baseline after an overnight fast of 12 hours. Cases and controls also received standard laboratory testing. The concentrations of serum fast blood glucose (FBG), TC, total TGs, HDL and LDL were measured using an enzymatic colorimetric assay. Lp(α), Serum ApoA1 and ApoB levels were measured using the immune turbidimetric method. Uric acid (UA) was measured using uric acid enzymatic methods. The metabolite profiles were performed on ABBOTT ARCHITEC c16000 (Chicago). The intra- and inter-assay coefficients of variation for all measurements were 5% and 10%, respectively. The ratios of these markers including the ratio of TG to HDL (R-TG/HDL), the ratio of TC to HDL (R-TC/HDL), the ratio of LDL to HDL (R-LDL/HDL), the ratio of ApoB to ApoA1 (R-ApoB/ApoA1) and the ratio of ApoA1 to ApoB (R-ApoA1/ApoB), were calculated.

Culture of human ectopic endometrial stromal cells

With permission of the patients, lesion tissues from the 8 patients whose intraoperative r-ASRM scores were all endometrial stage 3/4 were sampled under sterile conditions and kept in cold DMEM/F-12 (Gibco) with 1:100 Penicillin-Streptomycin Liquid (Beyotime) for subsequent cell culture. The tissues were digested with 0.2% type I collagenase (Solarbio) in 37^{O}C for 1.5 hours and then hand filtered using a 70 μM cell filter (BD Falcon). Cells were cultured in DMEM/F-12 with 10% FBS (Gibco) and 1% Penicillin-Streptomycin Liquid in an incubator (Esco) at 37^{O}C, 5% CO2. The cells were passaged when the density of primary cells had reached more than 75%. Resveratrol (Selleck) was initially dissolved in DMSO (Sangon) to make 20 mM and 8 mM mother fluids, and then diluted to the working concentrations of 100 μM and 40 μM, respectively.

Lipidomics analysis

Sample preparation and detection: Eight groups of the cultured primary HEcESCs were divided into two parts. One was treated with 100 μM resveratrol and the other was treated with solvent only. Culturing was for 48 hours where about 1 × 10^{6} cells were collected and subjected for the following lipidomic analysis. All samples were prepared according to previously described techniques (22). An UHPLC system was used to coordinate an electrospray ion source using a Q Exactive-HF MS system (Thermo) which was used for lipid profiling (UPLC-MS). Chromatographic conditions: Flow rate was 0.26 mL/min while column temperature was 55^{O}C. The mobile phases consisted of (A) 60% acetonitrile/H_2O with 10 mM ammonium and (B) Isopropanol: acetonitrile = 9:1 (with 10 mM ammonium format). We applied positive and negative mode linear gradients to detect the subjects, respectively. Mass spectrometry was performed using a Thermo Q ExactiveTM benchtop Orbitrap mass spectrometer equipped with heated ESI source in ESI positive and negative modes (Thermo).

Data Processing: All assay raw data were collected using Xcalibur data acquisition software (Thermo). The data, including m/z-values, retention times, and peak areas, were extracted using LipidSearch software (Thermo). All of the detected lipids were quantified using the Thermo TraceFinderEFS software (version 3.2). The lipid molecules were named by reference to the LipidMaps website. We enabled One-MAP (www.5omics.com) software to support comprehensive metabolic data analysis. Multivariate statistical analysis was performed online. This included hierarchical clustering analysis, Pearson correlation heat maps, Z-score plot, Volcano plot, principal component analysis (PCA), partial least squares discriminant analysis (PLS-DA), orthogonal partial least squares discriminant analysis (OPLS-DA), construction of a receiver operating characteristic curve (ROC) univariate, and the construction of a permutation plot and a variable importance in projection (VIP) plot.

Cell proliferation, invasiveness and apoptosis assays

Proliferation: Cultured HEcESCs, grown to the logarithmic growth stage, were digested with 0.25% Trypsin-EDTA and re-suspended. 100 μL of 4 × 10^{4} cells/mL suspension was inoculated into 96-well plates (Corning) for 24 hours. Four experimental groups, each with triplets, were prepared as follows: blank (100 μL culture medium); control (DMSO); Re-40 μM (resveratrol at a concentration of 40 μM); Re-100 μM (resveratrol at a concentration of 100 μM). After 48 hours treatment, 10 μL CCK8 (Solarbio)

solution was added and incubated for another 4 hours. The cell viability was measured with a BioTek Synergy 1 plate reader (BioTek) and calculated.

Invasiveness: The matrigel (Solarbio) was thawed at 4^{O}C and diluted with 1: 12 in serum-free DMEM/F-12. The 8 μM upper chamber of the transwell plates (Corning) was coated and gelatinized for 1 hour in an incubator at 37^{O}C. The cells were treated with DMSO, 40 μM resveratrol and 100 μM resveratrol for 48 hours and then digested. The upper chambers were filled with 2×10^4 cells in 1% FBS DMEM/F-12 medium and the lower chamber with 600 μL 10% FBS DMEM/F-12 medium. The triple transwell plates were placed at 37^{O}C, in a 5% CO_2 incubator for 48 hours. Transwell chambers were fixed with 95% ethanol and stained with 0.1% crystal violet for 30 minutes. Five visual fields (400×) were randomly selected under the microscope to count the cells that had crossed the matrigel.

Apoptosis: The cells were treated separately with DMSO, 40 μM resveratrol or 100 μM resveratrol for 48 hours, then digested and re-suspended using a binding buffer (Beyotime) to make a 1×10^6 cells/mL suspension. 100 μL cell suspension was added into a 5 mL flow tube and 5 μL Annexin V Alexa Fluor 488 was then added. The mixture was incubated in a dark room for 5 minutes and 10 μL PI, 200 μL PBS was then added. Cellular apoptosis was analyzed by NovoCyte Flow cytometer (ACEA).

Establishment of a rat model of EMs and medical treatment

Animals: Fifty female Sprague Dawley rats aged 8–10 weeks, weighing 200–250 g, were placed in a clean-level environment in the Zhejiang University Laboratory Animal Center with 12 hours light/dark cycles and regular feeding. Animal experimental methods and purposes were all in line with ethical standards and international practices.

Modeling: Prior to any surgery, the estrous cycle stages of female rats were examined using vaginal biopsy samples. Attrition cells, showing as irregular keratinocyte like cells and gathered together on the slides, was considered to be an indicator of a mature estrous stage for efficient EMs modeling. Rats having a 4–5 days estrous cycle and two consecutive estrus cycles were then selected for surgery. The animals were anesthetized using 45 mg/kg by intraperitoneal injection of 3% pentobarbital (BIOCAM) sodium and operated under strict aseptic conditions at a room temperature of 28-30^{O}C. Rat estrus epithelial tissue with a 0.8×0.8 cm^2 endometrium was auto-transplanted into the endometrial abdominal wall. Welfare nursing was provided after the operation. Ten rats were also selected for a placebo operation to serve as sham. The animals were fed regularly for 4 weeks.

Examination: A laparotomy was performed 4 weeks after the surgery. The rats were euthanized and the laparotomy was performed to measure size of the implant. Modeled rats were recorded and the lesion volume was calculated using the following formula: $V = a \times b^2/2$ (a represents the broadest transverse diameter of the lesion, b represents the vertical diameter line) and $V \geq 2$ mm^3 was considered as a successful model.

Resveratrol treatment and evaluation

Resveratrol was dissolved in 35% DMSO for intraperitoneal injection in rats, while the Sham group and EMs group were injected with the same amount of the solvent (0.9% NaCl + 35% DMSO). Thirty rats with successful modelling were divided into three groups randomly: EMs group (n = 10), Res-med group (n = 10, resveratrol dose = 15 mg/Kg/d), Res-high group (n = 10, resveratrol dose = 45 mg/Kg/d). The rats of four groups were administered continuously for 28 days. Lesions were examined (as above method). Lesion tissues and blood were sampled before and after resveratrol treatment for evaluation.

HE staining

Lesion tissues were fixed in 10% formalin and dehydrated with a gradient of alcohol for paraffin slicing. The sections were processed according to a standard protocol for staining with Hematoxylin and Eosin (Solarbio). Images were taken under a light microscope (Nikon) and pathological features were analyzed.

Detection of serum TC, TG, HDL and LDL of rat models

Whole blood (500 μL) was collected and centrifuged to detect TC, TG, HDL and LDL and analyzed by fully automatic biochemical analyzer (Toshiba FR120). The following Detection kit (Beijian) were used: total cholesterol measurement kit (CHOD-PAP method); low-density lipoprotein cholesterol measurement kit (direct method-protective reagent method); high-density lipoprotein cholesterol measurement kit (Direct method-selective inhibition method); Triglyceride kit (GPO-PAP).

qRT-PCR

Total RNAs were extracted from tissues or cells using trizol (Sangon) and then reversely transcribed into cDNA using a reverse transcription kit (Vazyme). ChamQSYBRqPCR Master Mix (Vazyme) was applied for qRT-PCR using a real-time quantitative PCR machine HT faster 9600T (Biosystem). The following primers were used: β-actin-F: 5’-ATCCGTAAAGACCTCTATGC-3’, R: 5’-ACACAGAGTACTTGCGCTCA-3’; PPARα-F: 5’-GGCAATGCACTGAACATCGAG-3’, R: 5’-GAAAGCCGCTTGATAAGCCG-3’.

Western blot

Total proteins were extracted using a standard protein lysis buffer. The protein concentration was determined using a BCA kit (Gene Ray). The standard curve was made according to the absorption value of standard liquid, and the concentration of protein was measured and calculated. Samples were subjected to SDS-PAGE and transferred to a polyvinylidene fluoride membrane. Membranes were immunoblotted with rabbit anti-PPARα (1:500, Proteintech) and mouse anti-Actin (1:1000, Goodhere Biotechnology Co, AB-M-M001). Detection of proteins was performed using the ChemiLucentTM ECL detection reagents (Millipore, WBKLS0500). Images were taken using the chemiluminescence imaging system (Clinx Science Instruments).

The open field assay

The open field experiment was carried out in a market equipment (open square box, 2 m × 2 m × 50 cm) which was equipped with an infrared camera (CCTVLENS). Experiments were performed in the standard manner. The rats were placed in the test room to acclimatize for 2 hours, and then each one placed in the

same orientation when entering into the market. The test time of each rat was 5 minutes. The trajectory and movements of the rats was tracked using Video Track 3.10 software for subsequent analysis of parameters such as the movement time in the central area and the number of entrances into the central area. In between each experiment the field was cleaned with 70% ethanol to eliminate the odour of the previous rat.

Statistics

Continuous characteristics were presented as Means ± SD for normal variables, and Median (Q1-Q3) for abnormal variables. The difference between control groups and the EMs group for different phenotypes was tested by ANOVA and T-test for normal variables, Kruskal-Wallis test and Wilcoxon test for abnormal variables. Categorical variables were given as N (%) and the chi-square test was applied to compare the distributions across different groups. Multivariable logistic models were applied to assess the association of Metabolite indicators with EMs in general, and with its two phonotypes more specifically.

As potential risk factors, all above interesting metabolite markers, plus general information including age, BMI, history of delivery and abortion, were entered into the initial model. A step-wise selection method, with a significance level of 0.05 required to allow a variable into the model (SLE = 0.05), and 0.10 for a variable to remain in the model (SLS = 0.10), was then adopted to identify the final model which contains the best subset of the potential risk factors. Finally, for each single variable, as well as for the union of variables in the final model, ROC curves were performed to determinate the diagnostic value where Youden index (sensitivity + specificity-1) was used to select best cut-off point. Statistical analyses were conducted using SAS, version 9.4 (SAS Institute, Cary, NC). The difference between the two groups was analyzed using a T test (Graphpad Prism5). Differences were considered significant at a p-value of < 0.05, marked $*P < 0.05$, $**P < 0.01$, $***P < 0.001$.

Abbreviations

Area under a curve AUC

Apolipoprotein A Apo A

Apolipoprotein B Apo B

Confidence interval CI

Ceramide Cer

Deep infiltrating endometriosis DIE

Diacylglycerol DG

Endometriosis EMs

Ectopic endometrial stromal cells HEcESCs

Fast blood glucose FBG

Fatty acid anion FA

Fold Change FC

High-density lipoprotein HDL

High-density lipoprotein cholesterol HDL-C

Low-density lipoprotein LDL

Lipoprotein α Lp(α)

Lysophosphatidylthanolamine LPE

Low-density lipoprotein cholesterol LDL-C

Lysophosphatidylcholine LPC

Monoacylglycerol MG

Ovarian endometriosis OMA

Orthogonal partial least squares discriminant analysis O-PLS-DA

Principal component analysis PCA

Partial least squares discriminant analysis PLS-DA

Phosphatidylinositol PI

Phosphatidyl glycerol PG

Phosphatidylserine PS

Phosphatidylcholine PC

Phosphatidyl ethanolamine PE

Receiver operating characteristic curve ROC

Resveratrol Res

Sphingomyelin SM

Triglyceride TG

Total cholesterol TC

Uric acid UA

Very low-density lipoprotein VLDL

Variable Importance in Projection VIP

Declarations

Ethics approval and consent to participate

The experimental and required specimen collections were reviewed and approved by the Ethics Committee of Women's Hospital School of Medicine Zhejiang University, and all the participants signed their written informed consent before the study. All animal experiments were approved by the Zhejiang University Experimental Animal Welfare Ethics Review Committee.

Consent for publication

The manuscript has been approved by all authors.

Availability of data and material

The datasets used or analysed during the current study are available from the corresponding author on reasonable request.

Competing interests

The authors have declared that no conflict of interest exists.

Funding

This work was funded by National Key R&D Program of China (2017YFC1001202, 2018YFC1004900), Zhejiang Bureau of Traditional Chinese Medicine (2017ZA092), and Zhejiang National Science Foundation (LGF20H040010, LY17H040004).

Authors' contributions

Y.X, Z.C. and M.G designed research studies and interpreted data. Z.C., C.W, and C.L acquired and analyzed data; C.W, C.L., H.Z., Y.Z. and X.L. performed experiments; Y.X., Z.C., C.L., X.Y and X.Z., developed the methodology and provided the reagents; Z.C. C.W. and C.L. wrote the initial draft. Y.X. and M.G revised the manuscript. All authors contributed helpful suggestions for this manuscript.

Acknowledgements

We thank Shiyu. Shi and Aiming. Chen from Dalian ChemDataSolution Information Technology Co. Ltd for the metabolomics validation analysis. We are very grateful to Minchao. Li for helping on clinical data analysis and to Chris Wood from the Life Science College of Zhejiang University for valuable discussion and language support. Thanks also to Xiangwei. Fei and the Laboratory Animal Center of Zhejiang University and Core Facilities, Zhejiang University School of Medicine for technical support.

References

1. Han SJ, Jung SY, Wu SP, Hawkins SM, Park MJ, Kyo S, Qin J, Lydon JP, Tsai SY, Tsai MJ, DeMayo FJ, O'Malley BW. Estrogen Receptor β Modulates Apoptosis Complexes and the Inflammasome to Drive the Pathogenesis of Endometriosis. *Cell* (2015); 163: 960-974.
2. Chapron C, Fritel X, Dubuisson JB. Fertility after laparoscopic management of deep endometriosis infiltrating the uterosacral ligaments. *Human reproduction (Oxford, England)* (1999); 14: 329-332.
3. Kohl Schwartz AS, Wölfler MM, Mitter V, Rauchfuss M, Haeberlin F, Eberhard M, von Orelli S, Imthurn B, Imesch P, Fink D, Leeners B. Endometriosis, especially mild disease: a risk factor for miscarriages. *Fertility and sterility* (2017); 108: 806-814.e802.
4. Guo S-W. Recurrence of endometriosis and its control. *Human Reproduction Update* (2009); 15: 441-461.
5. Liu Y, Zhang W. Association between body mass index and endometriosis risk: a meta-analysis. *Oncotarget* (2017); 8: 46928-46936.
6. Lafay Pillet MC, Schneider A, Borghese B, Santulli P, Souza C, Streuli I, de Ziegler D, Chapron C. Deep infiltrating endometriosis is associated with markedly lower body mass index: a 476 case-control study. *Human reproduction (Oxford, England)* (2012); 27: 265-272.
7. Crook D, Howell R, Sidhu M, Edmonds DK, Stevenson JC. Elevated serum lipoprotein(a) levels in young women with endometriosis. *Metabolism: clinical and experimental* (1997); 46: 735-739.
8. Melo AS, Rosa-e-Silva JC, Rosa-e-Silva AC, Poli-Neto OB, Ferriani RA, Vieira CS. Unfavorable lipid profile in women with endometriosis. *Fertility and sterility* (2010); 93: 2433-2436.
9. Fless GM, Juhn D, Karlin J, Rubenstein A, Scanu AM. Response of rhesus serum high density lipoproteins to cycles of diet-induced hypercholesterolemia. *Arteriosclerosis (Dallas, Tex)* (1984); 4: 154-164.
10. Gibran L, Maranhão RC, Tavares ER, Carvalho PO, Abrão MS, Podgaec S. mRNA levels of low-density lipoprotein receptors are overexpressed in the foci of deep bowel endometriosis. *Human Reproduction* (2017); 32: 332-339.
11. Hoover-Plow J, Hart E, Gong Y, Shchurin A, Schneeman T. A Physiological Function for Apolipoprotein(a): A Natural Regulator of the Inflammatory Response. *Experimental Biology and Medicine* (2009); 234: 28-34.
12. Lu BC, Zhang XM. [Associations of metabolism of lipid, calcium and phosphate in endometriosis]. *Zhonghua fu chan ke za zhi* (2008); 43: 185-188.

13. Yang L, Li M, Shan Y, Shen S, Bai Y, Liu H. Recent advances in lipidomics for disease research. *Journal of separation science* (2016); 39: 38-50.
14. Stevens KG, Bader CA, Sorvina A, Brooks DA, Plush SE, Morrison JL. Imaging and lipidomics methods for lipid analysis in metabolic and cardiovascular disease. *Journal of developmental origins of health and disease* (2017); 8: 566-574.
15. Vouk K, Hevir N, Ribić-Pucelj M, Haarpaintner G, Scherb H, Osredkar J, Möller G, Prehn C, Rižner TL, Adamski J. Discovery of phosphatidylcholines and sphingomyelins as biomarkers for ovarian endometriosis. *Human reproduction (Oxford, England)* (2012); 27: 2955-2965.
16. Chagovets VV, Wang Z, Kononikhin AS, Starodubtseva NL, Borisova A, Salimova D, Popov IA, Kozachenko AV, Chingin K, Chen H, Frankevich VE, Adamyan LV, Sukhikh GT. Endometriosis foci differentiation by rapid lipid profiling using tissue spray ionization and high resolution mass spectrometry. *Scientific reports* (2017); 7: 2546.
17. Adamyan LV, Starodubtseva N, Borisova A, Stepanian AA, Chagovets V, Salimova D, Wang Z, Kononikhin A, Popov I, Bugrova A, Chingin K, Kozachenko A, Chen H, Frankevich V. Direct Mass Spectrometry Differentiation of Ectopic and Eutopic Endometrium in Patients with Endometriosis. *Journal of minimally invasive gynecology* (2018); 25: 426-433.
18. Braga D, Montani DA, Setti AS, Turco EGL, Oliveira-Silva D, Borges E, Jr. Metabolomic profile as a noninvasive adjunct tool for the diagnosis of Grades III and IV endometriosis-related infertility. *Molecular reproduction and development* (2019); 86: 1044-1052.
19. Li J, Gao Y, Guan L, Zhang H, Sun J, Gong X, Li D, Chen P, Ma Z, Liang X, Huang M, Bi H. Discovery of Phosphatidic Acid, Phosphatidylcholine, and Phosphatidylserine as Biomarkers for Early Diagnosis of Endometriosis. *Frontiers in physiology* (2018); 9: 14.
20. Huminiecki L, Horbańczuk J. The functional genomic studies of resveratrol in respect to its anti-cancer effects. *Biotechnology advances* (2018); 36: 1699-1708.
21. Prysyazhna O, Wolhuter K, Switzer C, Santos C, Yang X, Lynham S, Shah AM, Eaton P, Burgoyne JR. Blood Pressure-Lowering by the Antioxidant Resveratrol Is Counterintuitively Mediated by Oxidation of cGMP-Dependent Protein Kinase. *Circulation* (2019); 140: 126-137.
22. Lagouge M, Argmann C, Gerhart-Hines Z, Meziane H, Lerin C, Daussin F, Messadeq N, Milne J, Lambert P, Elliott P, Geny B, Laakso M, Puigserver P, Auwerx J. Resveratrol improves mitochondrial function and protects against metabolic disease by activating SIRT1 and PGC-1alpha. *Cell* (2006); 127: 1109-1122.
23. Tsai HY, Ho CT, Chen YK. Biological actions and molecular effects of resveratrol, pterostilbene, and 3'-hydroxypterostilbene. *Journal of food and drug analysis* (2017); 25: 134-147.
24. Simental-Mendía LE, Guerrero-Romero F. Effect of resveratrol supplementation on lipid profile in subjects with dyslipidemia: A randomized double-blind, placebo-controlled trial. *Nutrition (Burbank, Los Angeles County, Calif)* (2019); 58: 7-10.
25. Vuralli D, Wattiez AS, Russo AF, Bolay H. Behavioral and cognitive animal models in headache research. *The journal of headache and pain* (2019); 20: 11.

26. Gupta D, Hull ML, Fraser I, Miller L, Bossuyt PM, Johnson N, Nisenblat V. Endometrial biomarkers for the non-invasive diagnosis of endometriosis. *The Cochrane database of systematic reviews* (2016); 4: Cd012165.
27. Wang C, Jin A, Huang W, Tsang LL, Cai Z, Zhou X, Chen H, Chan HC. Up-regulation of Bcl-2 by CD147 Through ERK Activation Results in Abnormal Cell Survival in Human Endometriosis. *The Journal of clinical endocrinology and metabolism* (2015); 100: E955-963.
28. Oka S, Alcendor R, Zhai P, Park JY, Shao D, Cho J, Yamamoto T, Tian B, Sadoshima J. PPARα-Sirt1 complex mediates cardiac hypertrophy and failure through suppression of the ERR transcriptional pathway. *Cell metabolism* (2011); 14: 598-611.
29. Zarzuelo MJ, López-Sepúlveda R, Sánchez M, Romero M, Gómez-Guzmán M, Ungvary Z, Pérez-Vizcaíno F, Jiménez R, Duarte J. SIRT1 inhibits NADPH oxidase activation and protects endothelial function in the rat aorta: implications for vascular aging. *Biochemical pharmacology* (2013); 85: 1288-1296.
30. Koninckx PR, Ussia A, Adamyan L, Wattiez A, Gomel V, Martin DC. Pathogenesis of endometriosis: the genetic/epigenetic theory. *Fertility and sterility* (2019); 111: 327-340.
31. Bruner-Tran KL, Osteen KG, Taylor HS, Sokalska A, Haines K, Duleba AJ. Resveratrol inhibits development of experimental endometriosis in vivo and reduces endometrial stromal cell invasiveness in vitro. *Biology of reproduction* (2011); 84: 106-112.
32. Schmelz EM, Dillehay DL, Webb SK, Reiter A, Adams J, Merrill AH, Jr. Sphingomyelin consumption suppresses aberrant colonic crypt foci and increases the proportion of adenomas versus adenocarcinomas in CF1 mice treated with 1,2-dimethylhydrazine: implications for dietary sphingolipids and colon carcinogenesis. *Cancer research* (1996); 56: 4936-4941.
33. Dillehay DL, Webb SK, Schmelz EM, Merrill AH, Jr. Dietary sphingomyelin inhibits 1,2-dimethylhydrazine-induced colon cancer in CF1 mice. *The Journal of nutrition* (1994); 124: 615-620.
34. Varga T, Czimmerer Z, Nagy L. PPARs are a unique set of fatty acid regulated transcription factors controlling both lipid metabolism and inflammation. *Biochimica et biophysica acta* (2011); 1812: 1007-1022.
35. Park HS, Lim JH, Kim MY, Kim Y, Hong YA, Choi SR, Chung S, Kim HW, Choi BS, Kim YS, Chang YS, Park CW. Resveratrol increases AdipoR1 and AdipoR2 expression in type 2 diabetic nephropathy. *Journal of translational medicine* (2016); 14: 176.
36. Bäck M, Yurdagul A, Jr., Tabas I, Öörni K, Kovanen PT. Inflammation and its resolution in atherosclerosis: mediators and therapeutic opportunities. *Nature reviews Cardiology* (2019); 16: 389-406.
37. He D, Zhao M, Wu C, Zhang W, Niu C, Yu B, Jin J, Ji L, Willard B, Mathew AV, Chen YE, Pennathur S, Yin H, He Y, Pan B, Zheng L. Apolipoprotein A-1 mimetic peptide 4F promotes endothelial repairing and compromises reendothelialization impaired by oxidized HDL through SR-B1. *Redox biology* (2018); 15: 228-242.

38. Kravitz MS, Pitashny M, Shoenfeld Y. Protective molecules–C-reactive protein (CRP), serum amyloid P (SAP), pentraxin3 (PTX3), mannose-binding lectin (MBL), and apolipoprotein A1 (Apo A1), and their autoantibodies: prevalence and clinical significance in autoimmunity. *Journal of clinical immunology* (2005); 25: 582-591.
39. Yu Q, Zhang Y, Xu CB. Apolipoprotein B, the villain in the drama? *European journal of pharmacology* (2015); 748: 166-169.
40. Xuan Q, Hu C, Yu D, Wang L, Zhou Y, Zhao X, Li Q, Hou X, Xu G. Development of a High Coverage Pseudotargeted Lipidomics Method Based on Ultra-High Performance Liquid Chromatography-Mass Spectrometry. *Analytical chemistry* (2018); 90: 7608-7616.

Tables

Due to technical limitations, table PDFs are only available as a download in the Supplemental Files section.

Figures

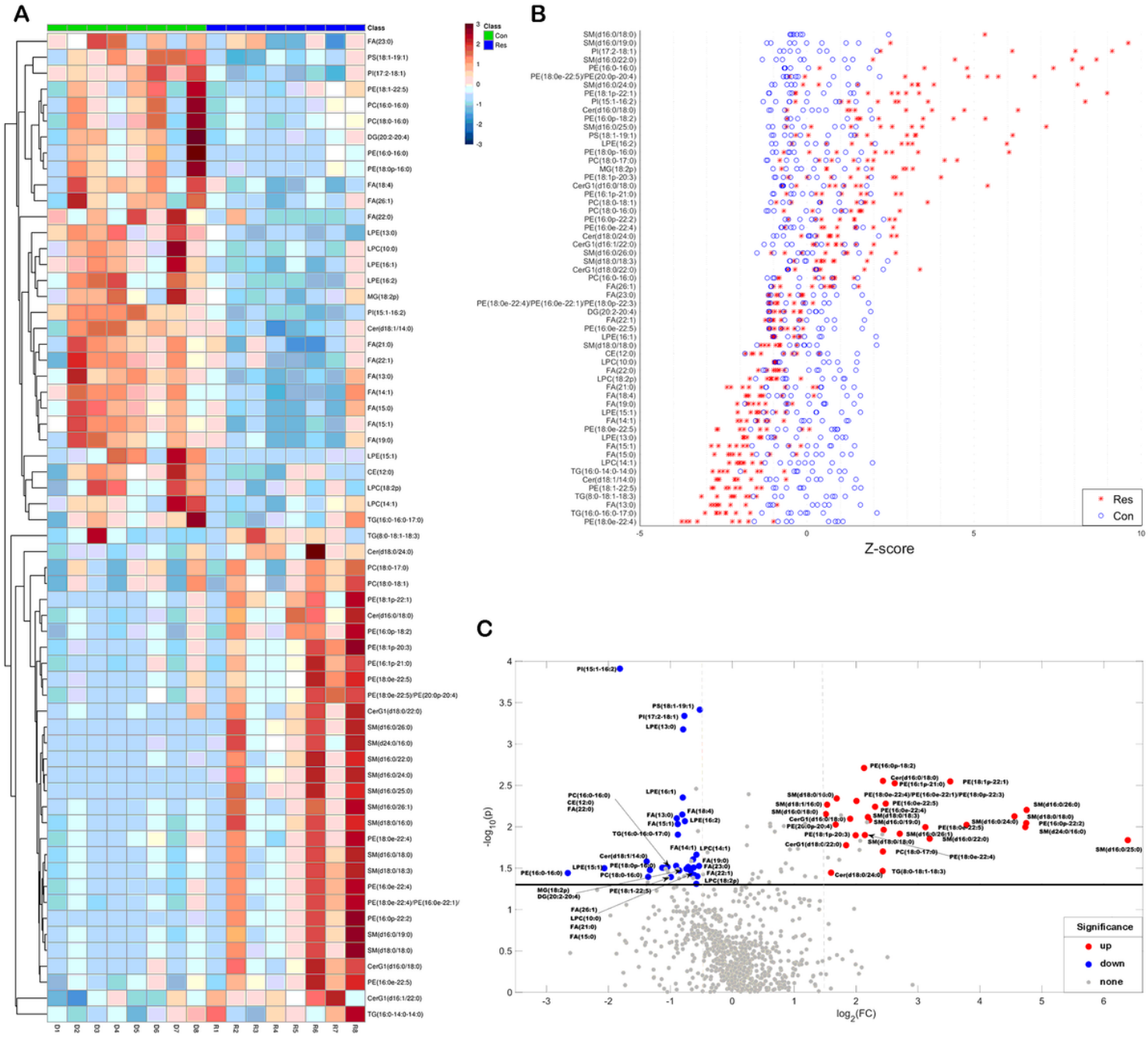

Figure 1

Lipidomics analysis on HEcESCs treated with or without resveratrol. (A). Heatmap representation of analytes in HEcESCs (n=8) and HEcESCs treated with resveratrol (n=8). Color scale indicates the relative richness of lipid metabolites. (B) Z-score quantification of lipids detected in both HEcESCs (Con) and HEcESCs treated with resveratrol (Res). A positive z-score suggests possible upregulation, while a negative z-score suggests possible downregulation. (C) Volcano plot showing analytes that were increased (red) or decreased (blue) in HEcESCs after resveratrol treatment compared with HEcESCs without resveratrol treatment.

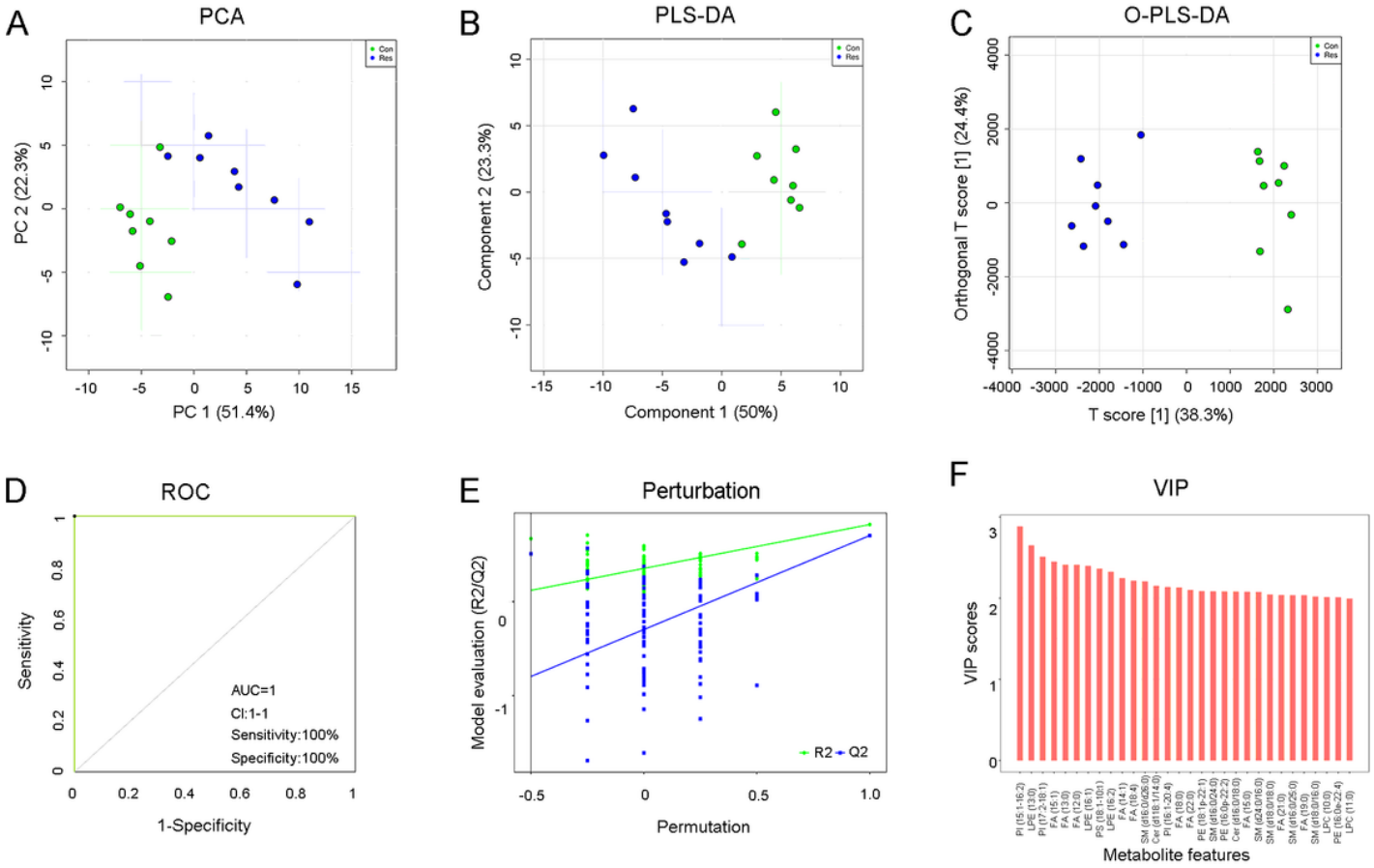

Figure 2

Multivariate statistical analysis. (A) Principal component analysis (PCA) and clustering for HEcESCs samples from Con and Res. PCA score plot across the first 2 components created using log-transformed feature intensities across all metabolite features. (B) Partial least squares discriminant analysis (PLS-DA) of HEcESCs lipid profiles, 2D score plot. (C) Orthogonal projections to latent structures discriminant analysis (OPLS-DA) of HEcESCs samples (Con and Res). (D) ROC analysis was used to examine the property of the OPLS-DA model with AUC=1. (E) The permutation plot showing the best predictability and reliability of OPLS-DA model. (F) VIP plot. Metabolites were ranked according to their increasing importance to group separation between Control (Con) and Resveratrol treatment (Res).

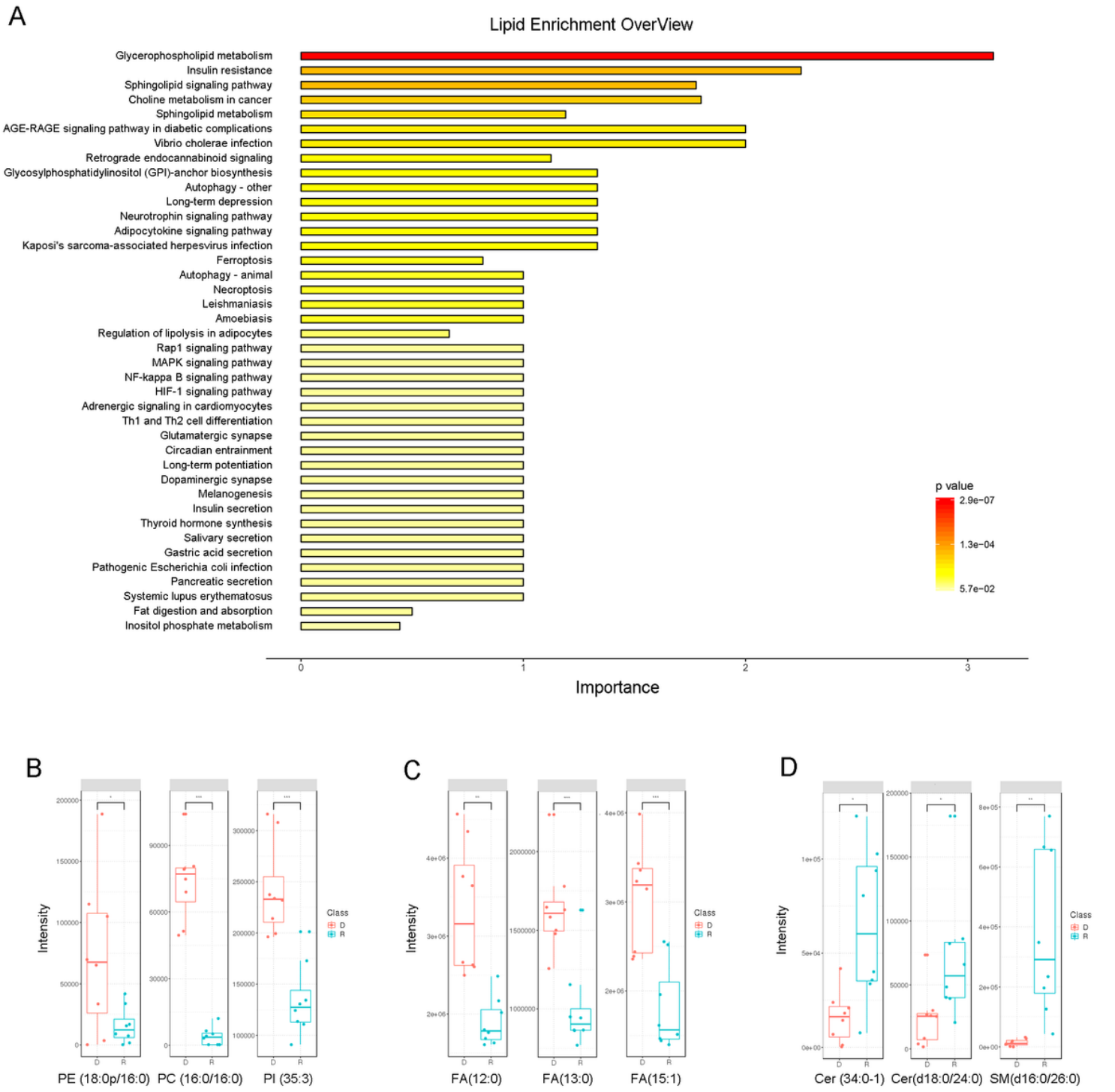

Figure 3

Lipid-associated signaling pathways affected by resveratrol treatment. (A) The altered lipid metabolites (under either VIP>1, P<0.05 or FC>1.5criteria) were subjected to the KEGG database for pathway enrichment analysis. The block represents the p-value of the indicated pathways. The lipidomic changes upon resveratrol treatment were mostly assigned to the glycerophospholipid metabolism pathway, insulin resistance pathway or sphingolipid signaling pathways, among all related pathways (Table. S1). (B-D)

showing key lipids FA (B), PE, PC and PI (C), Cer and SM (D) in the related signaling pathways, that have been significantly altered upon resveratrol treatment.

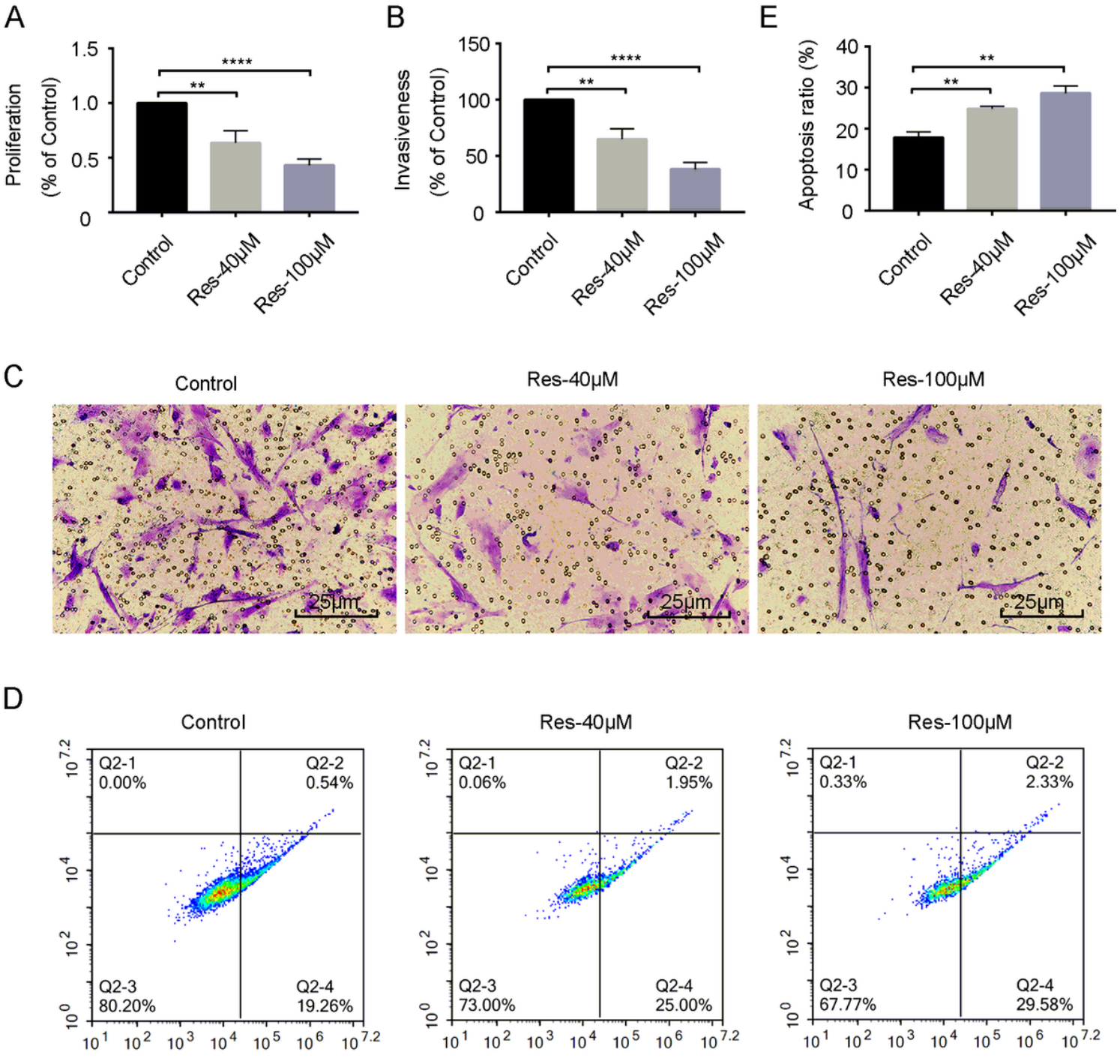

Figure 4

Effects of resveratrol on cell proliferation, invasiveness and apoptosis in HEcESCs. (A) After 48 hours treatment with resveratrol at different concentrations (Res-40 μM and Res-100 μM), the proliferation capacity of the HEcESCs had decreased by 36.30% in the Res-40 μM group and 57.78% in the Res-100 μM group, compared with the control groups, with significant differences. (B-C) In the invasiveness assay, from the same amount of cells (2x104), the number of cells crossing the matrigel differed significantly

with resveratrol treatment at a concentration of 40 μM or 100 μM, which were decreased by 35.00% and 61.72% respectively, compared to the control group. (D-E) The effects of resveratrol on the apoptosis of HEcESCs. The proportion of early apoptosis in the control group was 19.26%, which increased to 25.00% after treatment with 40 μM resveratrol, and to 29.58% after treatment with 100 μM resveratrol for 48 hours, both showing significant differences.

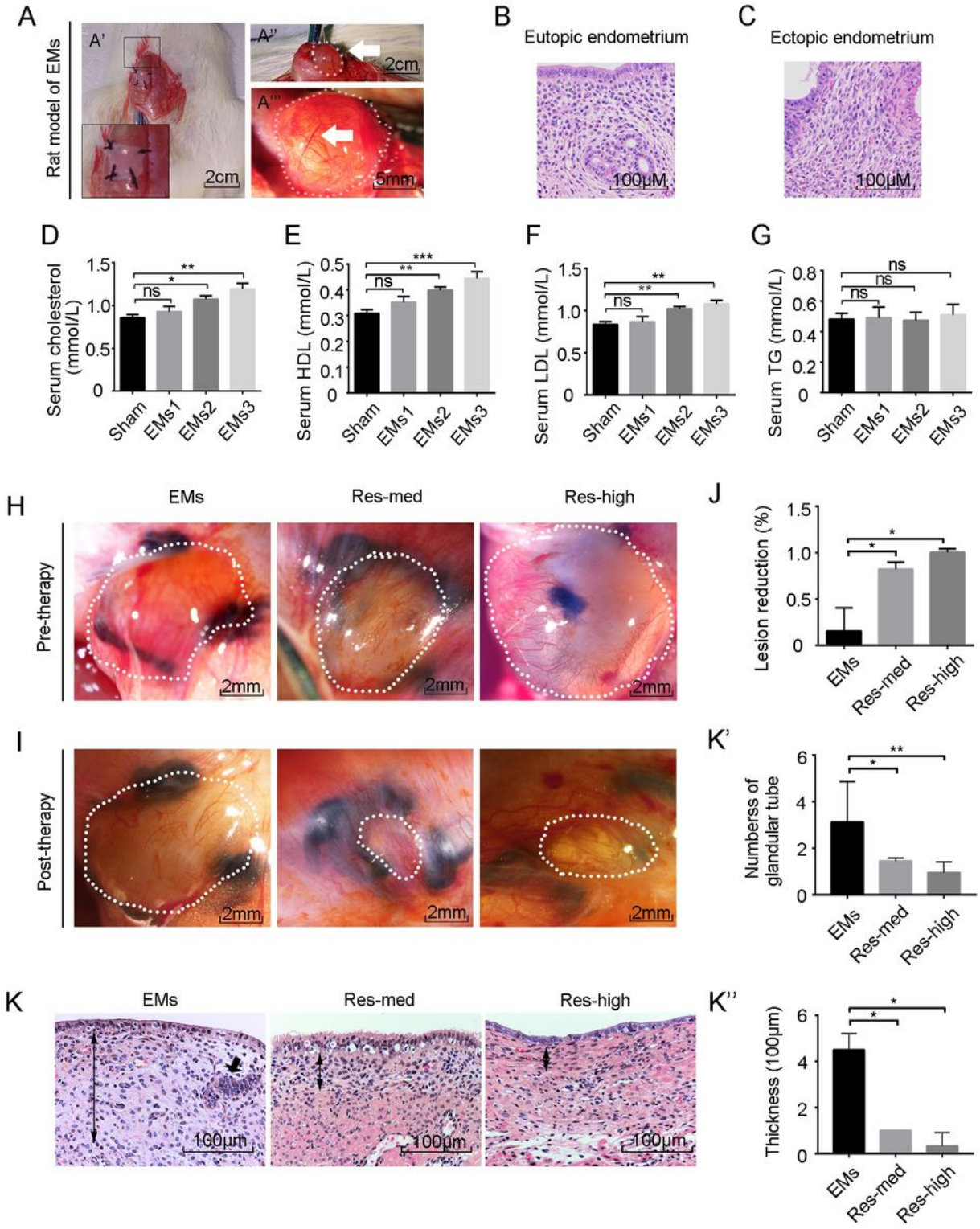

Figure 5

Resveratrol attenuated the lesions of endometriosis model rats. (A) Autotransplantation of rat endometrium into the abdominal wall was performed under strict aseptic conditions (A'). After 4 weeks of modelling, successful implants showed EMs-like lesions appearing as vesicular cysts, filled with clear or turbid yellow-brown liquid (A", arrow) and surrounded by connective tissue and angiogenesis (A"', arrow). (B-C) HE staining showed the implant-derived ectopic endometrium was similar to the eutopic endometrium. (D-G) Metabolic profiles in the groups of rat models and the sham group (control) were measured and analyzed. Serum levels of cholesterol (D), HDL (E), LDL (F), and TG (G) were classified in the model animals according to three levels: 2 mm3≤EMs 1<20 mm3, 20 mm3≤EMs2<100 mm3 or EMs 3≥100 mm3, (each n≥5). There were no significant differences in serum CHOL, HDL, LDL or TG observed between the EMs 1 group (2 mm3≤volume<20 mm3) and the sham group. The levels of serum CHOL, HDL, LDL but not TG were significantly increased in both EMs2 and EMs3 groups (≥20 mm3), compared to the controls. (H-I) The lesions in the rat models were measured pre-treatment (H), and re-measured after 4 weeks of resveratrol treatment in the Res-med group (n=10, resveratrol dose=15 mg/Kg/d), Res-high group (n=10, resveratrol dose=45 mg/Kg/d), and EMs group (DMSO, n=10) (I). (J) The volume of lesions were calculated and statistic analyzed. Significant reduction of lesion sizes were shown in both Res-med groups and Res-high groups, compared to the EMs group without resveratrol treatment. (K-K") HE staining of lesion samples in EMs, Res-med and Res-high groups, showing a decrease in both thickness (arrows) (K') and glandular tube (arrowheads) of the ectopic endometrium (K").

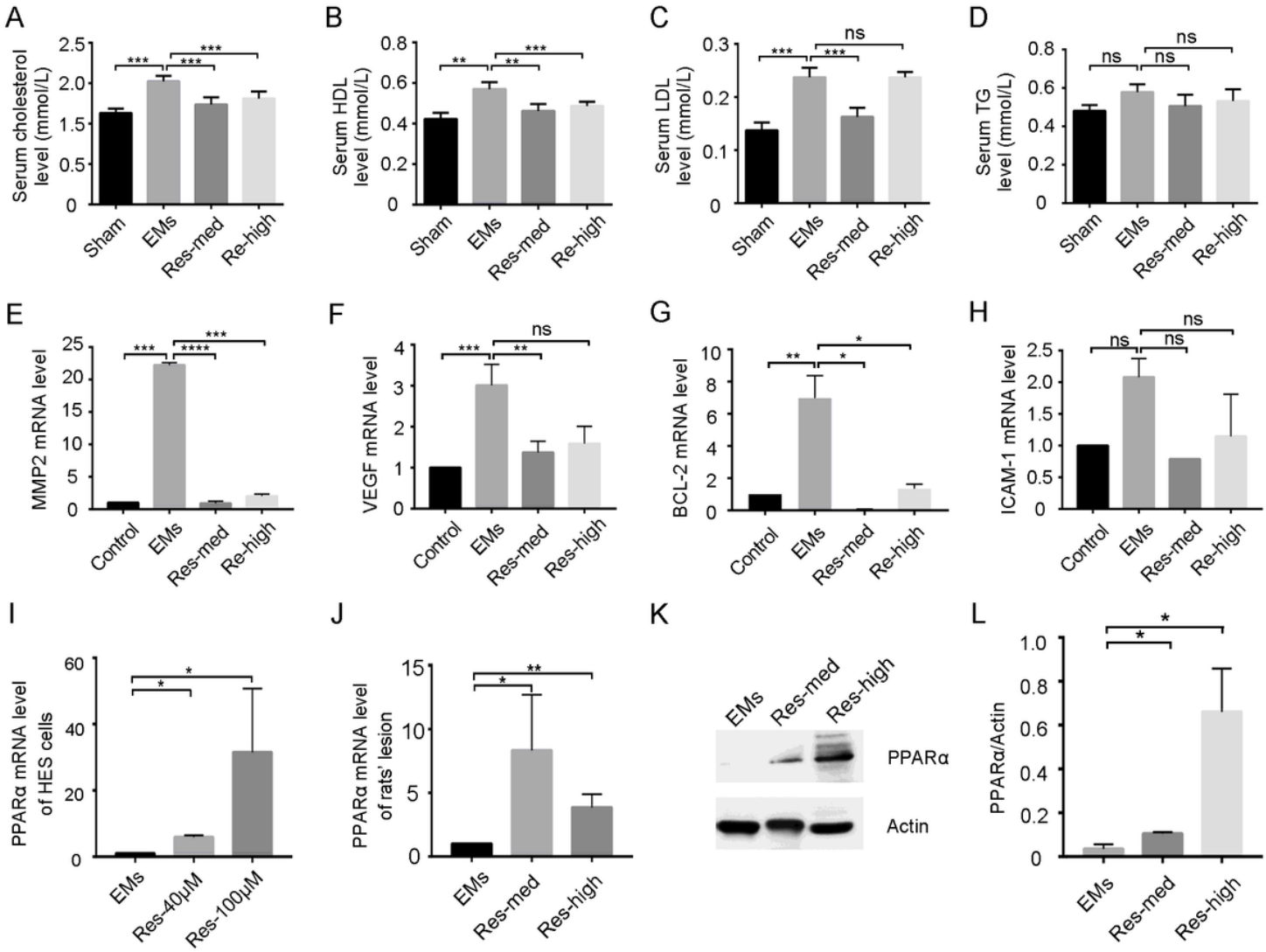

Figure 6

Resveratrol treatment modulated aberrant lipid profiles and related gene expressions. (A-D) Metabolite profile alterations upon resveratrol treatment in rat models. The levels of serum cholesterol (A), HDL (B) and LDL(C) showed significant decreases in the Res-med groups and cholesterol (A), HDL (B), but not LDL(C) showed significant decrease in the Res-high groups, compared to the EMs group without resveratrol treatment. No significantdifferences in the levels of TG were observed between any groups (D). (E-H) mRNA levels of MMP2 (E), VEGF (F), BCL-2(G) and ICAM1 (H) in ectopic endometrial lesions and upon resveratrol treatment were analyzed. Significant increases in the mRNA levels of MMP2, VEGF and Bcl-2 were detected in the lesions of EMs groups, compared to the control animals (E-G). The mRNA levels of MMP2, VEGF and Bcl-2 were significantly decreased in Res-med groups, compared to EMs groups (pre-treatment models). The mRNA levels of MMP2 and Bcl-2, but not VEGF were significantly decreased in Res-high groups, compared to EMs groups (pre-treatment models). No significantdifferences in mRNA levels of ICAM-1 were observed between any of the experimental groups (H). (I-L) After resveratrol treatment, significant increases in mRNA levels of PPARα were detected in both HEcESCs of patients (I) and the ectopic endometrial tissues of rat models (J) compared to the endometrial tissues

without resveratrol treatment. (K-L) Western blot showed that PPARα expressions were significantly increased in the Res-med group and the Res-high group after resveratrol treatment, compared to the EMs groups.

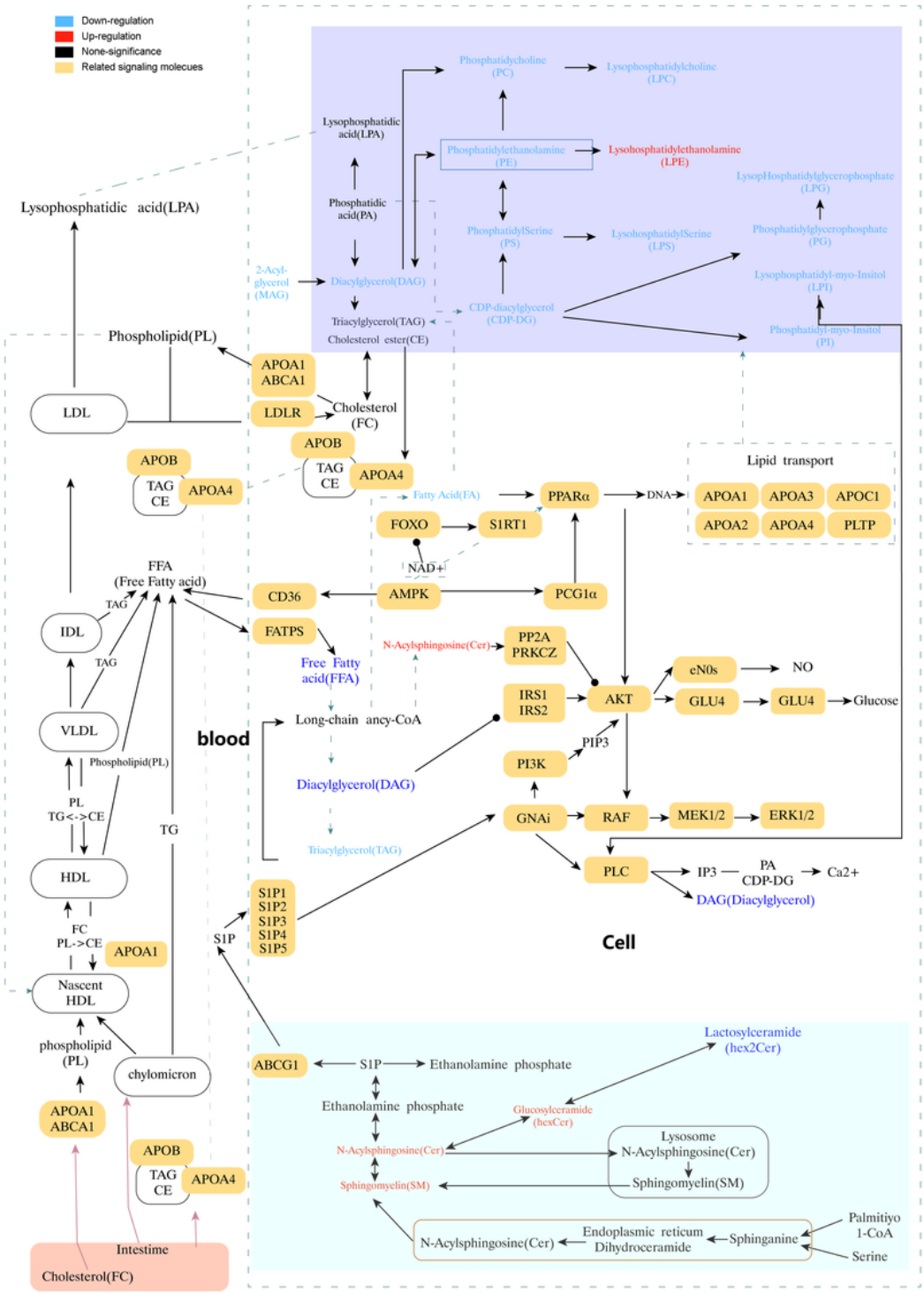

Figure 7

Lipid-mediated mechanisms upon resveratrol treatment in HEcESCs. Resveratrol mediated lipidomic alterations may interplay in a dynamic network contributing to attenuate pathologies associated with

EMs through possible effects on cell proliferation, apoptosis and anti-inflammation. Resveratrol triggered lipid-associated signaling pathways and molecular networks are revealed mainly in three clusters: (1) The glycerolphospholipid metabolism pathway (upper panel), showing PC, PE, PS and CDP-DAG are down-regulated, resulting in reduced PI and PG synthesis. These glycerolphospholipids play important roles in transmembrane transport of substances between blood and peripheral cells. (2)The glycerolipid related insulin-resistance (IRS) pathway (middle panel), showing that resveratrol mediated reduction of FA could stimulate AMPK and PPARα activation. Resveratrol mediated down-regulation of DAG might directly activate IRS/PI3K-AKT pathways. These factors in turn could influence the regulation of lipid transport genes and inflammatory responses. (3) The sphingolipid metabolism pathway (lower panel), showing that the synthesis of the sphingolipids Cer and SM are significantly increased. This may affect cell proliferation and apoptosis. The words in a blue represent down-regulated lipids, in red, up-regulated lipids, and in black, lipids without significant changes. Yellow shading represents related signaling molecules.

Supplementary Files

This is a list of supplementary files associated with this preprint. Click to download.

- SupplementaryFiguresandTables.pdf
- Table1.pdf
- Table2.pdf